Ziyan_WU 6521805

by Ziyan WU

Submission date: 23-Jun-2020 08:35AM (UTC+0100)
Submission ID: 131006724
File name: 171907_Ziyan_WU_Ziyan_WU_6521805_4224217_2141028067.pdf (1.44M)
Word count: 6224
Character count: 30849



Department of Mechanical, Materials & Manufacturing Engineering

BEng Individual Project
MMME3023

Large Eddy Simulation of Bubble Column Two-Phase Bubbly Flow with Considerations of Different Interfacial Forces

Ziyan WU

6521805

Professor Xiaogang Yang

Submitted in part for the BEng degree in Mechanical Engineering

2019/20

1. Abstract

In this dissertation, large eddy simulation of a laboratory-scale bubble column two-phase bubbly flow with considerations of different interfacial forces is presented. The simulation generally follows Sanyal's experimental specification. The large eddy simulation (LES) with the two-fluid Euler-Euler approach is adopted as the turbulence model to simulate the gas-liquid two-phase bubbly flow. The influence of interfacial forces: drag force, lift force and virtual mass force under the condition of LES on the axial liquid velocity profile and radial gas hold up profile is investigated. The Ishii Zuber and Schiller Naumann drag force model, Tomiyama lift force model is adopted for simulation respectively according to previous experiences of papers. It can be concluded that: (1) LES model can capture the details of fluid transient flow, which provides a more comprehensive understanding of bubble column. (2) An obvious optimization on the prediction of axial water velocity can be obtained when considering virtual mass force and lift force. (3) Although both Ishii Zuber drag force model and Schiller Naumann drag force model can capture the general shape of the both water velocity and gas holdup distribution profile, there is still some discrepancy between them and the experimental data.

2. Introduction

Bubble column is widely used in chemical industry, biological pharmacy, metallurgy and other fields because of its characteristics of good heat and mass transfer *[1-2]*. The main advantages of bubble column are that there are no moving parts in a bubble column, and it is easy to conduct maintenance *[3]*. It provides the slow liquid phase reaction with large interface area, high transfer rate between gas and liquid phase and large liquid holdup *[4]*.

In recent years, computational fluid dynamics (CFD) has been increasingly applied to the study of complex fluid dynamics in bubble column *[5]*. However, how to describe the interaction between gas and liquid and the adoption of the turbulence model rationally are the critical and difficult points for CFD simulations to reproduce the complex flow state in the bubble column. Therefore, more and more researches on the physical models describing the momentum exchange between the phases including drag force, lift force and virtual mass force of the bubble column have emerged in recent years. Lift force is one of the factors that influence flow, but many researchers choose to ignore lift when simulating a bubble column because of the uncertainty in choosing the value of lift coefficient *[6]*. For the virtual mass, most researchers believe that the it has no significant influence on the simulation results except Mudde and Simonin *[7]*.

Many researchers have conducted experiments and simulations on the influences of drag force. For example, Li et al. *[8]* and Pfleger et al. *[9]* used Grace drag model to conduct gas-liquid two phase simulation of a bubble column and both get satisfactory results. Muhammad et al. *[10]* used the Schiller Naumann drag model to study the effects of different distributors in the bubble column and obtained reasonable results. From the aspect of Ishii Zuber drag model, Zhang et al. *[11]* compared the Tomiyama closed drag model with the Ishii drag model and found that the calculated results of the Tomiyama model were consistent with the experimental values. Although the influence of drag model on the simulation results has been reported in the literature, it is important to consider the combination of the turbulence model and the drag model since the influence of drag force is also included in the equation of the two phase turbulence model.

Most of the researchers choose to use $k-\varepsilon$ model as the turbulence model. For example, In Sanyal et al.'s *[12]* experiment, the adopted turbulence model is $k-\varepsilon$

model. $k-\varepsilon$ model is based on the time averaging, only the average motion parameters and the statistical average parameters of a few pulsations are involved, which can be used to predict macroscopic large scale phenomena. However, the generation, development and structure of the two-phase turbulence cannot be predicted. As the standard $k-\varepsilon$ model is derived, the turbulence is assumed to be fully developed and the molecular viscosity is assumed to be neglected. Therefore, the $k-\varepsilon$ model is only applicable to the case where turbulence is fully developed. DNS (Direct Numerical Simulation) can realize the simulation of small scale vortexes and obtain the details of turbulence generation and development. However, the amount of computer storage and calculation required for DNS is too large. According to Bao *[13]*, the whole three-dimensional space will have at least ${R_L}^{9/4}$ grid points. Thus, DNS can only be adopted when the Reynolds number is around medium, and the geometric boundary is simple.

The emergence of large eddy simulation (LES) becomes a bridge connecting the large scale simulation and small scale simulation. It directly solves the filtered N-S equation under the grid system of large scale vortex while the small scale vortex can be simulated by the relationship between the Subgrid Scale model and the large vortex. The filtering operation is equivalent to weighted averaging of the function in a certain range in a certain way. Its function is to filter out the high wave number and only keep the low wave number. The wavelength of truncated wave number is determined by the characteristic size of the filtering function. Compared with the $k-\varepsilon$ model, which only solves the velocity fluctuation over a long period of time, the LES model can capture the strong transient movement of bubbles, and it is in good agreement with the experimental data. N.G.Deen et al. *[14]* used LES model to simulate the gas-liquid flow in a square sectioned bubble column. After comparing with the experimental data, it is found that the simulation carried out by LES can capture the strong instantaneous

motion information of the bubble flow and the velocity data is also consistent with the measure values. When the simulation is transient, LES is supposed to describe velocity profile better than $k-\varepsilon$ model. Because the fluctuation of velocity is caused by the pulsating velocity of the liquid, $k-\varepsilon$ model is difficult to obtain the details of the high frequency pulsation of the fluid velocity while LES can capture the instantaneous amount of fluid at any point in the bubble column at any given moment.

The simulation is based on the experimental system of Sanyal et al. *[12]* and uses large eddy simulation as the turbulence model. The influence of interfacial forces under LES on numerical simulation of bubble column two-phase bubbly flow is investigated. Three cases are respectively set up, whose settings are essentially the same except momentum transfer settings. The first case, which is named *case 1* in the later section, adopts Ishii Zuber drag force model and chooses to neglect lift force and virtual mass force. The second case, which is named *case 2* in the later section, adopts Schiller Naumann drag force model and chooses to neglect lift force and virtual mass force. The third case (named *case 3* in the later section) adopts Schiller Naumann drag force model, considering the effects of lift force and virtual mass force. Tomiyama model is adopted to describe the lift force. The transient characteristics of radial gas hold up and axial flow rate of liquid are investigated, by comparing the simulation results of three cases.

3. Numerical Model Description

3.1 Governing equation

The simulation adopts the Euler-Euler two-fluid approaches to describe the gas-liquid two phases in the bubble column and there are continuity equation and momentum equation for the gas-liquid two phase, without mass transfer between the phases.

Mass conservation equation

$$\frac{\partial(\rho_i \alpha_i)}{\partial t} + \nabla \cdot (\rho_i \alpha_i \vec{u}_i) = 0 \quad (1)$$

Momentum conservation equation

$$\frac{\partial(\alpha_i \rho_i \vec{u}_i)}{\partial t} + \nabla \cdot (\alpha_i \rho_i \vec{u}_i \vec{u}_i)$$

$$= -\nabla(\alpha_i \mu_i \overline{S}_i) - \alpha_i \nabla p + \alpha_i \rho_i g + F_{i,I} - \nabla \cdot \alpha_i \tau_i \quad (2)$$

Where,

the lower index i represents the different phases: gas and liquid;

α_i represents the volume fraction of the phase i;

ρ_i represents the density of the phase i;

μ_i represents the molecular viscosity of the phase i;

$\vec{u}_i$ represents the resolved velocity;

τ_i represents the unresolved stress tensor;

If the index i turn to be g, it will designate the gas phase;

If the index i turn to be l, it will designate the liquid phase;

$F_{i,I}$ represents the sum of the two-phase momentum exchange including all interfacial forces such as drag force, lift force, wall lubrication, virtual mass force and dispersion force;

τ_i and $F_{i,I}$ need appropriate models to conduct the calculation, the models adopted are discussed below;

3.2 Turbulence Model

3.2.1 Model Theory

In this simulation, the adopted turbulence model is Large Eddy Simulation (LES). LES is to separate the large eddy from the small eddy in turbulence and directly solve

the large eddy through the N-S equation. The small eddy can be simulated by establishing the subgrid scale model and thus connected with large eddy. The structure of large vortexes in liquid flow and gas movement as well as the details of liquid turbulence caused by bubbles can be given through LES. LES can capture the strong instantaneous motion information of the bubble flow compared with the k-ε model.

Turbulent contains vortices of different time and length scales. The maximum length scale is usually the characteristic length of the average flow, and the minimum scale is the Kolmogrov scale. LES choose a filter width to filter the governing equations between the large scale structure and small scale structure. This specified scale is called Kolmogorov scale. Thus, all the variables are divided into large scale and small scale. The large scale is directly simulated while the small scale is simulated by adopting subgrid model. The filtering process is to get rid of the vortex smaller than the filter width or a given physical width, so as to get the governing equation of the large vortex.

The nature of turbulence can be summarized in the following aspects: three-dimensional, unsteady (varying over time), multiscale. As a result, direct simulation of turbulence calculation takes a high computational cost. To simulate turbulence with limited computer resources, several methods were proposed including LES and RANS (Reynolds averaging). Averaging can be used to derive the terms in equation (1) and (2). It is worth noting that a similar form of the equation will be found if filtering is used for further derivation of the equation. To explain this, the difference between basic ideas of LES and RANS needs to be investigated. The difference is that LES carries out filtering to N-S equation and then only calculate the large-scale turbulence and the turbulence smaller than the filtering scale is described by the model while RANS is to average the N-S equation by time and transform the unsteady turbulence problem into a steady problem at the cost of the appearance of additional unknowns. Mathematically,

turbulence smaller than the filter scale is represented by the additional stress terms, known as the subgrid stress. Existing turbulence theories have concluded that almost all turbulence has some similarity on sufficiently small scales. In essence, LES is still a simulation of unsteady turbulence but the calculation scale is relaxed. RANS substantially changes the problem by abandoning the simulation of unsteady turbulence information and seeking only flow results of averaging. Although LES and RANS differ greatly in their ideas, the filtering equation solved by LES and the time averaging equation solved by RANS is very similar in mathematical form, and the subgrid stress and the Reynolds stress are also completely corresponding in mathematical form.

3.2.2 Basic equations of LES

In this simulation, the process of treating different phases of turbulence varies. A simple zero equation model is adopted for the turbulence of dispersed gas since the gas has a relatively low density. For the continuous liquid phase, LES is adopted.

The filtering variable is defined as (The horizontal line):

$$\bar{\phi}(x) = \int_D \phi\,(x')G(x,x')dx' \tag{3}$$

Where,

D represents the fluid region;

G is the filter function that determines the size of the vortex.

The liquid velocity $\vec{u}_L$ in equation (1) and (2) represents the contribution of resolved velocity. Thus the corresponding unresolved part can be calculated by:

$$u'_L = u_L - \vec{u}_L \tag{4}$$

Where,

u_L represents the true velocity of liquid.

The SGS stress tensor can be represented by:

$$\tau_{ij} = \overline{u_i}\overline{u_j} - \overline{u_i} \cdot \overline{u_j} \quad (5)$$

3.2.3 Subgrid Model

The subgrid model was first proposed by Smagorinsky *[15]* and improved by Lilly *[16]*. The SGS stress tensor τ_{ij} is unknown and needs to be simulated to get a closed equation. Currently the most adopted subgrid model is in the form:

$$\tau^a{}_{ij} = \tau_{ij} - \frac{1}{3}\tau_{kk}\delta_{ij} = -2v_{sgs}\overline{S_{ij}} \quad (6)$$

Where,

$\tau^a{}_{ij}$ is the anisotropic part of the SGS tensor;

δ_{ij} is the Kronecker delta;

τ_{kk} is the trace of the SGS stress tensor, which can be added to a filtered pressure to calculate the modified pressure:

$$p = \bar{p} + \frac{1}{3}\tau_{kk}$$

$\overline{S_{ij}}$ is the strain rate tensor under the filtered scale, which is defined as:

$$\overline{S_{ij}} = \frac{1}{2}\left(\frac{\partial \overline{u_i}}{\partial x_i} + \frac{\partial \overline{u_j}}{\partial j}\right) \quad (8)$$

The subgrid turbulent viscosity v_{sgs} is a function expressed by the strain rate tensor $|\bar{S}|$, which can be calculated by:

$$v_{sgs} = \rho {L_s}^2 |\bar{S}| \quad (9)$$

Where,

$|\bar{S}| = \sqrt{2\overline{S_{ij}S_{ij}}}$;

L_s is the length scale of subgrid, can be calculated using the equation:

$$L_s = \min\left(kd, C_s V^{\frac{1}{3}}\right) \quad (10)$$

Where,

k=0.42 based on the formulation of Shur et al. *[17]*.

d is the distance to the closest wall;

V is the volume of the calculated control body;

C_s is the Smagorinsky constant, which is chosen to be $C_s = 0.1$ in this simulation. Van Driest model is adopted for the turbulence wall damping and the damping factor is assumed to be 25 by default.

In the aspect of bubble induced turbulence, the common BIT model of Sato et al. *[18]* is adopted to calculate the bubble influence on liquid turbulence. There is an additional extra term contributing to the SGS turbulent viscosity in this model,

$$\mu_{eff,l} = \mu_{mol,l} + \mu_{sgs,l} + \mu_{BIT,l} \tag{11}$$

Where,

$$\mu_{BIT,l} = C_B \rho_l \alpha_g d_B \left| u_g - u_l \right| \tag{12}$$

The constant C_B is set to be 0.6 and d_B represents the bubble diameter. According to T. Ma et al. *[19]*, $\mu_{BIT,l}$ can be directly added in this model without affecting the total turbulent kinetic energy, for example:

$$\tau^a{}_{ij} = \tau_{ij} - \frac{1}{3}\tau_{kk}\delta_{ij} = -2(v_{sgs} + v_{BIT})\overline{S_{ij}} \tag{13}$$

3.3 Drag Force Model

The two-phase momentum transfer term $F_{i,I}$ is mainly determined by the interaction forces, including drag force, lift force, virtual mass force and turbulence diffusion force etc. The drag force is numerically much larger than the other interfacial forces and cannot be ignored under any circumstances. The Ishii Zuber drag force model and Schiller Naumann drag force model are applied, which is respectively proposed by ISHII and ZUBER in 1979 *[20]*, Schiller and Naumann in 1935 *[21]*;

For a single bubble, its drag force in the static flow field is:

$$f_{g,D} = C_D \frac{\pi d_B}{4} \frac{1}{2} \rho |u_b - u_l|(u_b - u_l) \tag{14}$$

Where,

C_D represents the coefficient of drag force for single bubble.

Assuming that all bubbles in the cell are subjected to the same drag force per unit volume, the total drag force of all bubbles per unit volume is equal to the total number of bubbles in the cell multiplied by the equation (19):

$$F_{l,D} = -F_{g,D} = C_D \frac{\pi d_B}{4} \frac{1}{2} \rho |u_g - u_l|(u_g - u_l) \times \frac{\alpha_g}{\frac{\pi}{6} {d_B}^2}$$

$$= \frac{3}{4} \rho_l \alpha_g \frac{C_D}{d_b} |u_g - u_l|(u_g - u_l) \tag{15}$$

Where,

u_g represents the mass averaging velocity of the gas.

For C_D, different researchers have proposed different models.

3.3.1 Schiller Naumann drag model

$$C_D = \begin{cases} \frac{24(1+0.15Re^{0.687})}{Re} & Re \leq 1000 \\ 0.44 & Re > 1000 \end{cases} \tag{16}$$

3.3.2 Ishii Zuber drag model

$$C_D = \begin{cases} \frac{24(1+0.1Re^{0.75})}{Re} & Viscous \\ \frac{2}{3}\sqrt{Eo} & Distorted\ bubble \\ \frac{8}{3} & Spherical - cap\ bubble \end{cases} \tag{17}$$

Where, Eo is the Eotvos Number, which represents the ratio of the buoyancy to the surface tension of a bubble.

3.4 Lift Force Model

When bubbles move in a flow field with a velocity gradient, they will be affected by a force perpendicular to the direction of the relative velocity of bubbles and liquid flow filed, which is lift force. It includes the force caused by the uneven distribution of bubble surface pressure, the force caused by fluid shear movement, and the force caused by the uneven distribution of bubble rotation. The lift force can be represented by:

$$F_{l,L} = -F_{g,L} = C_L \rho_l \alpha_g \times (\nabla \times V_1) \tag{18}$$

Where, C_L is the lift force coefficient, which is related to the liquid viscosity, size and shape of bubbles. Tomiyama *[22]* thinks that shear stress and wake flow have the same formula for the effect on the buoyancy of bubbles. The influence of wake on the buoyancy force is considered by introducing an additional wake influence coefficient into the lift force coefficient. Tomiyama's model is shown as follows:

$$C_L = \begin{cases} \frac{\min\{0.288 \times \tanh[0.121 N_{Re}, f(N_{Eod})]\}}{Re} & For\ N_{Eod} < 4 \\ f(N_{Eod}) \end{cases} \tag{19}$$

It can be seen from the above equation that C_L contains two parts, namely the transverse force caused by shear stress and the buoyancy force caused by wake flow, which are respectively complex functions of Re number and Eo number.

3.5 Virtual Mass Force Model

Virtual mass force is caused by the fact that when the bubble accelerates relative to the liquid, the surrounding liquid is accelerated, making the bubble subject to additional mass force, which can be expressed as follows:

$$F_{l,VM} = -F_{g,VM} = C_{VM} \rho_l \alpha_g \times \left(\frac{D_g u_g}{Dt} - \frac{D_l u_l}{Dt}\right) \tag{20}$$

Where, C_{VM} is the virtual mass force coefficient, $\frac{D_g}{Dt}$ and $\frac{D_l}{Dt}$ respectively represents the derivatives of substances in the gas and liquid phases. Buwa et al. *[23]* choose the value of 0.5 for C_{VM} when simulating gas liquid two-phase flow in a bubble column. Cook et al. *[24]* choose the value of 0.25 for C_{VM} for the bubbles in water. In this simulation, C_{VM} is chosen to be 0.5, which is considered as rational for the simulation.

3.6 Numerical Procedure

3.6.1 Model grid establishment

Gambit 2.4.6 is used for the grid generation.

The objective of this simulation is specified by Sanyal's et al. *[12]* experiment. The simulation is performed for a 250.0 cm height air-water bubble column with a 19cm diameter. The 4 view is displayed in *figure 1*:

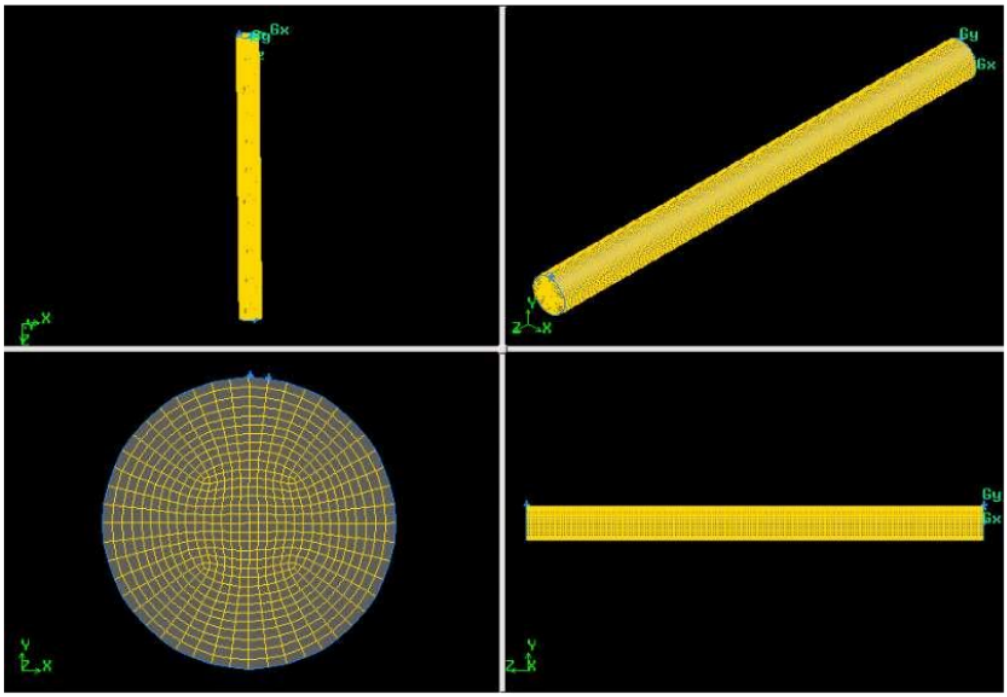


Figure 1: 4 view of the bubble column

There are total 156000 elements and the quality check result is shown in *Figure 2*:

```
Summarizing EQUISIZE SKEW of 3D elements measured for 1 meshed volume:
    Volume sanyal meshed using Cooper scheme and size of 1.000000.

  From value     To value     Count in range     % of total count (156000)
  ------------------------------------------------------------------------
           0           0.1           114899              73.65
         0.1           0.2            37799              24.23
         0.2           0.3              302               0.19
         0.3           0.4             3000               1.92
         0.4           0.5                0               0.00
         0.5           0.6                0               0.00
         0.6           0.7                0               0.00
         0.7           0.8                0               0.00
         0.8           0.9                0               0.00
         0.9             1                0               0.00
  ------------------------------------------------------------------------
           0             1           156000             100.00

  Measured minimum value: 0.00944637
  Measured maximum value: 0.37864

0 out of 1 meshed volume failed mesh check for skewed elements (EQUISIZE SKEW > 0.97).

0 out of 1 meshed volume failed mesh check for inverted elements.
```

Figure 2: mesh quality check using Equisize skew grid quality

3.6.2 CFD Settings

CFD commercial software CFX 2019 R3 is selected to perform transient simulation calculation.

Gas superficial velocity simulated is 12 cm/s, have the characteristic of churn-turbulent flow regime. The column contains a 95.0 cm high batch liquid, where the height is unexpanded. Three cases are respectively set up. The first case adopts Ishii Zuber drag force model and neglects lift force and virtual mass force. The second case adopts Schiller Naumann drag force model and neglects lift force and virtual mass force. The third case adopts Schiller Naumann drag force model, consider the effects of lift force and virtual mass force. Tomiyama model is adopted to describe the lift force.

The total time for three cases is the same: 100s. The time step is 0.001s, 0.005s and 0.005s respectively for the cases. The gas liquid phase is treated in the Euler-

Euler coordinate system. LES Smagorinsky is chosen for the turbulence model. For the advanced turbulence control, eddy viscosity is implemented through user defined functions:

```
LIBRARY:
  CEL:
    &replace EXPRESSIONS:
      EddyViscosity = (0.167*volcvol^(1/3))^2*(2*Shear Strain Rate*Shear Strain Rate)^0.5
*(1+0.7*AIR.vf*volcvol^(1/3)/0.005[m]*stokes^(3/2))*WATER.density
      InletVel = 0.4[m/s]*(1-((x^2+y^2)^0.5/0.075[m])^2)
      stokes = 1/(1+0.5)
      vfair = step((z-0.95[m])/1.0[m])
    END
  END
END
```

Smagorinsky model constant is set to be 0.1 by default. Van Driest model is adopted for the turbulence wall damping and the damping factor is assumed to be 25 by default. The fluid buoyancy model for both water and air is Density Difference. Surface tension coefficient for air and water is set to be 0.072 N/m, and Sato Enhanced Eddy viscosity is adopted for the enhanced turbulence production model. For the initialization, static pressure, velocity and volume fraction are all set to be automatic with value, which is both zero for static pressure velocity while for the volume fraction, it is implemented through user defined function *vfair*. For air, its value is *vfair* and thus *1-vfair* for water. The environment is assumed to me isothermal and fluid temperature is assumed to be 25 *Centigrade*. The reference pressure is 1 *atm*, air is assumed to be dispersed fluid with a 0.005m mean diameter and water is assumed to be continuous fluid. They both have a value -9.81 kg/m^3 in the Z direction for buoyancy model.

Central Difference is set to be advection Scheme and Second Order Backward Euler is set to be transient Scheme. The maximum number of iterations for each time step is *25* and *RMS* is used to be the convergence criteria to check the astringency with a residual target *0.0001*. A monitor point with the position *0.53 m* from the inlet

is set up to monitor the air velocity and air volume fraction. Every 100 timesteps, the *trn*. file is saved in case that the simulation is accidentally shut down.

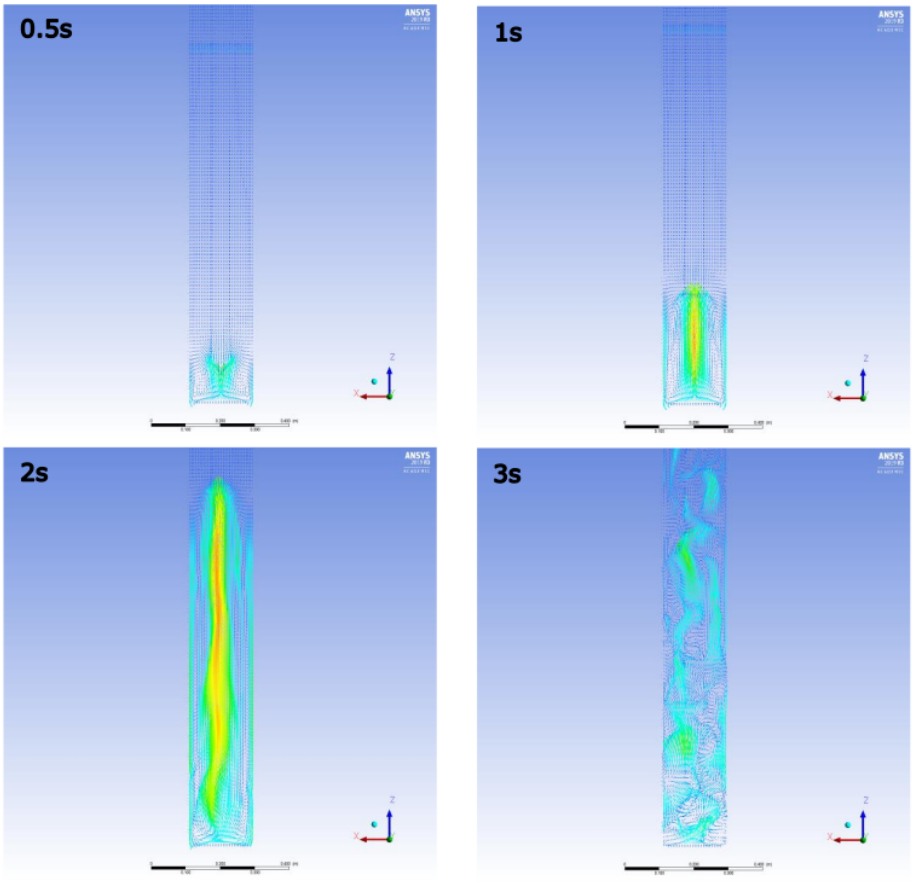
4. Results and Discussion

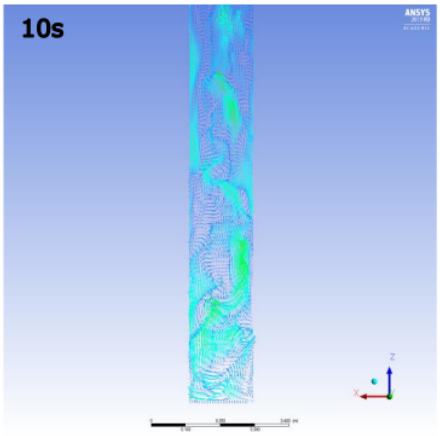
4.1 Axial Liquid Velocity

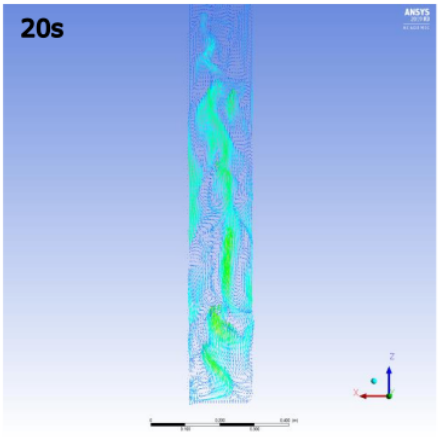
Figure series 3,4 below respectively shows projected vector distribution of the axial water velocity at *t=0.5, 1, 2, 3, 10, 20, 30, 50, 70, 80, 90, 100s* for *case 1* and *case 2* to investigate the influence of drag force model on axial liquid distribution, totally 12 small pictures.

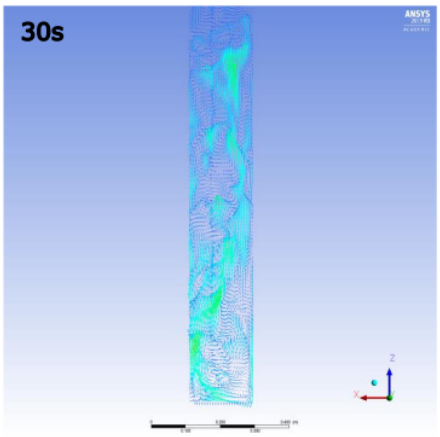
The projection plane is set at *ZX plane* and the range of velocity is *0 m/s – 3m/s*.

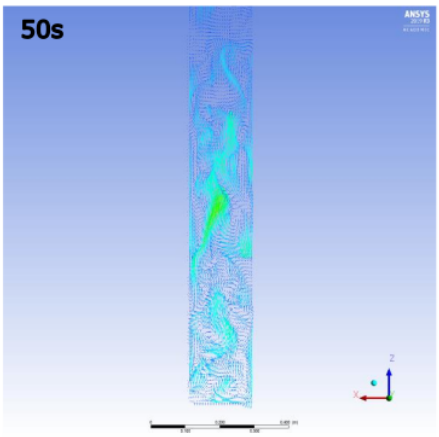
Figure series 3: axial water velocity for Case 1

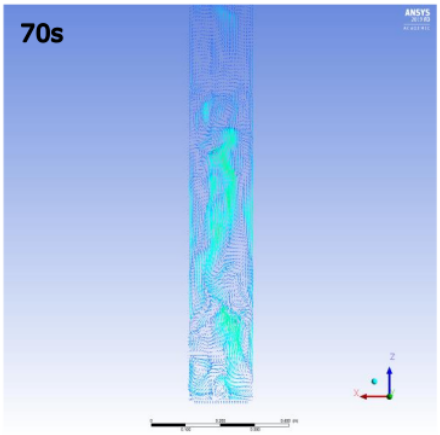


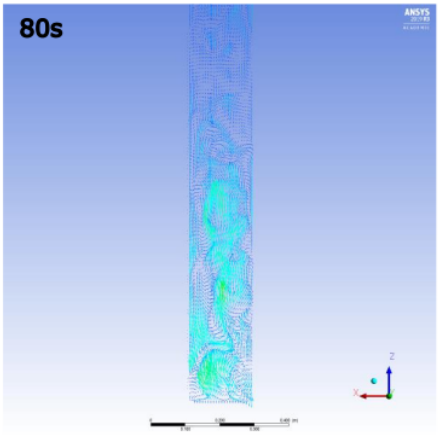

10s


20s


30s


50s


70s


80s

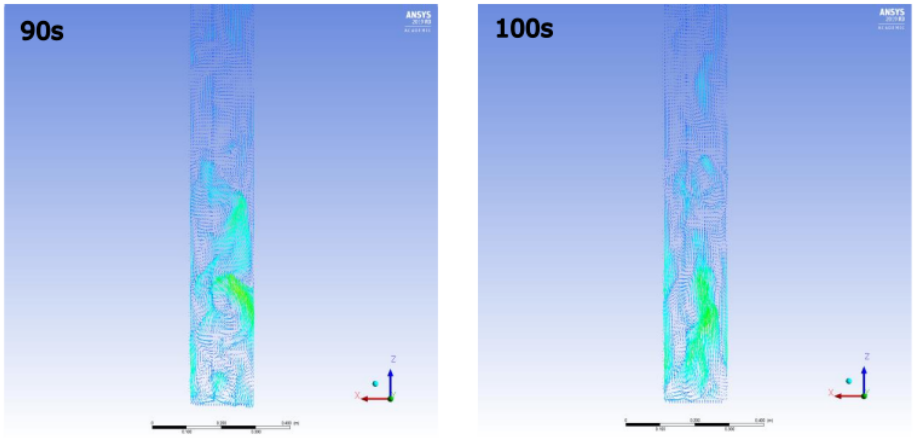
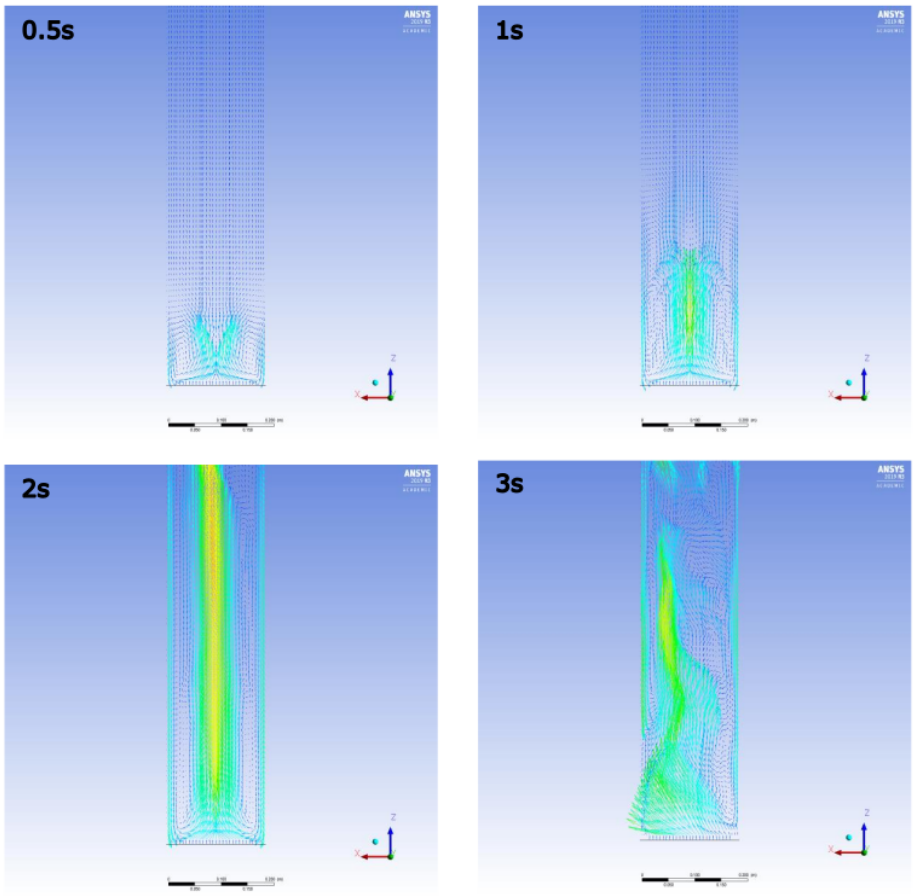
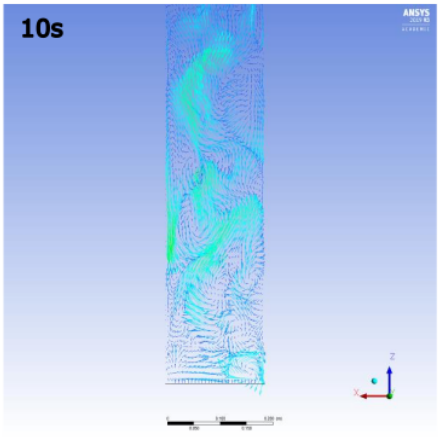
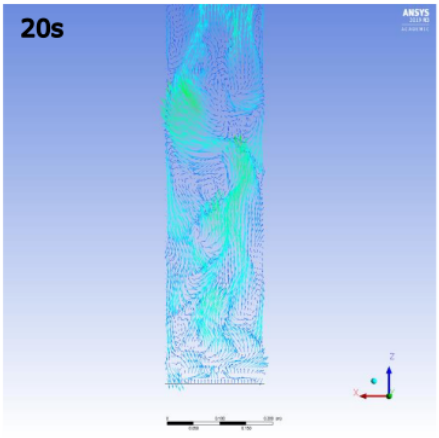
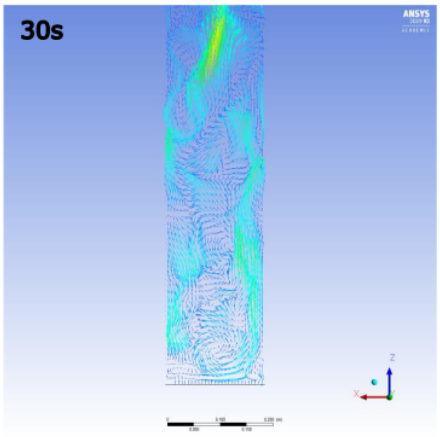


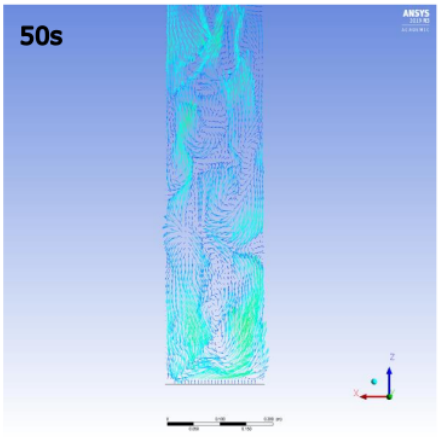
Figure series 4: axial water velocity Case for Case 2

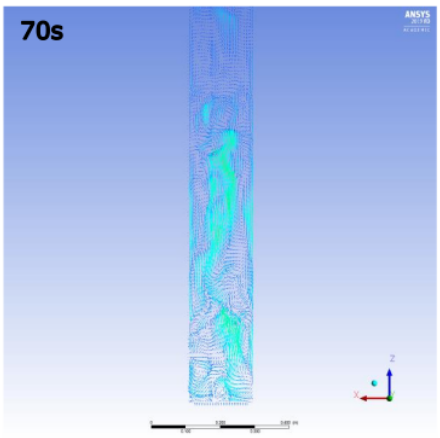


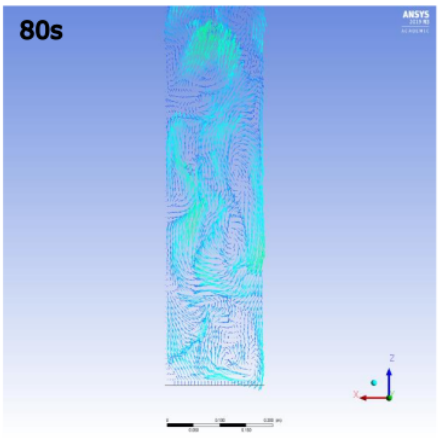

10s

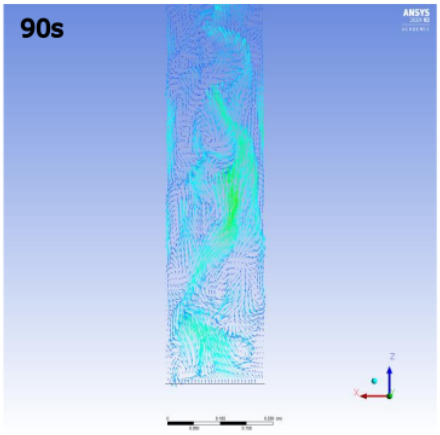

20s

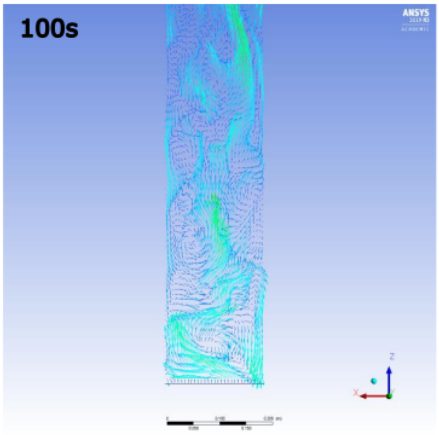

30s


50s


70s


80s





It can be seen from the study that in the initial stage of CFD research, people mainly focused on the average characteristics of flows. In the subsequent research progress, with the increase of computational force, the analysis of flow transient characteristic also became the focus of research. At present, there are many views on the fluid flow structure in bubble column. Stewart et al. *[25]* and Jakobsen et al. *[26]* conducted an in-depth study and review of the mean flow in the bubble column. These studies generally believe that the average flow shape within the bubble tower contains only a cyclic structure, with upward flow in the central region, downward flow near the wall and reverse flow only at the top and bottom of the tower. Therefore, most flows in the bubbling tower are axial flows, while radial flows only appear at the bottom of the bubble column.

Figure series 3 and 4 is the axial velocity vector distribution of liquid at the central section of the bubble column. It should be noted that because LES model can capture the details of fluid transient flow, the liquid level fluctuation caused by the initial gas inflow can be observed at t=1.0s, while the results obtained by k-ε cannot reflect the phenomenon at the initial stage of the intake. In fluid flow, buoyancy and drag force are two important factors of force balance in vertical direction, and drag

force acting on fluid element is the fundamental cause of continuous phase motion. From both figures it can be seen that after ventilation, the bubble flow rises at a low speed under the action of liquid resistance, thus driving the initial static liquid to move upward. Because of the conservation of liquid flow, liquid flows down near the wall, and the entire flow field shows an axisymmetric flow state. This phenomenon can be observed in both case 1 and 2. And this phenomenon fits well with the Sanyal's experiment data *[12]*.

At the same time, two vortex structures are developed on the left and right side of the flow. However, due to the space constraints, the scale is too small to see. At that place, the velocity gradient is large, leading the information of an upward pressure difference between the top and the bottom of the vortex, and the pressure difference makes the vortex rise. In the process of the motion of bubble flow, the vortex scale increases gradually until it reaches the liquid level. Because of the above two vortices mentioned, the whole flow field can still maintain a stable central axisymmetric flow mode for about 2 seconds. For each case, the symmetry disappears at t=3s. Then the transient instability of the side vortices of the bubble flow causes the force balance to be uneven in the horizontal direction. At $t=3s$, for *case 1* some large scale and high rotating speed vortexes collapse into smaller vortexes of the second order while *case 2* the large scale vortexes have not. Under the same vortex intensity, the smaller the scale of the vortex body is, the higher the frequency is. Therefore, the collapse process of a large vortex is also a transient process from a low-frequency vortex body to a high-frequency vortex body. In addition, the inertial effect of turbulence also trends to transfer energy to a high-frequency vortex body. The evolution of the visible vortex causes the bubble flow to migrate towards the side wall after a period of time. This motion of bubble flow is

intensified with the development of the vortices on the free interface, and the vortices move down along the left or right side of bubble flow with the time increasing. This phenomenon is much more obvious under *case 2* than *case 1*. Through these two figures, it shows that the axisymmetric flow structure in the bubble column is not invariable but develops with the flow and changes to show a random trend. The use of large eddy simulation helps us to capture the details of fluid transient flow at any moment with the maximum accuracy decided by the set fixed time step.

Figure 5 below presents the vector plot of the time-averaged water velocity under *case 1 and case 2*. The plane of the plot is at *ZX plane* and the reduction factor of the vector plot is set to be 3 to show the vector distribution more clearly. Through this figure, it shows that for both cases, after averaging the simulation results for a long time, the flow field in the bubble column will still be an approximately axisymmetric flow structure. The time-averaged water velocity profiles are qualitatively similar to the experimental flow profiles of Sanyal et al. *[12]*. It can be observed that the liquid rises along the centre axial of the bubble column and falls near the wall in a single loop. In contrast, real experiments are characterised by highly dynamic three-dimensional vortex bubbles that cause smaller bubbles and liquids to be dragged in their wakes. Form *figure series 3 and 4*, it can be shown that the transient flow in the three-dimensional bubble column is not an axisymmetric structure but contains a very obvious azimuth component. Therefore, the real motion of the rotating bubble group and the time scale of this phenomenon will be ignored by the axisymmetric model in *figure 5*.

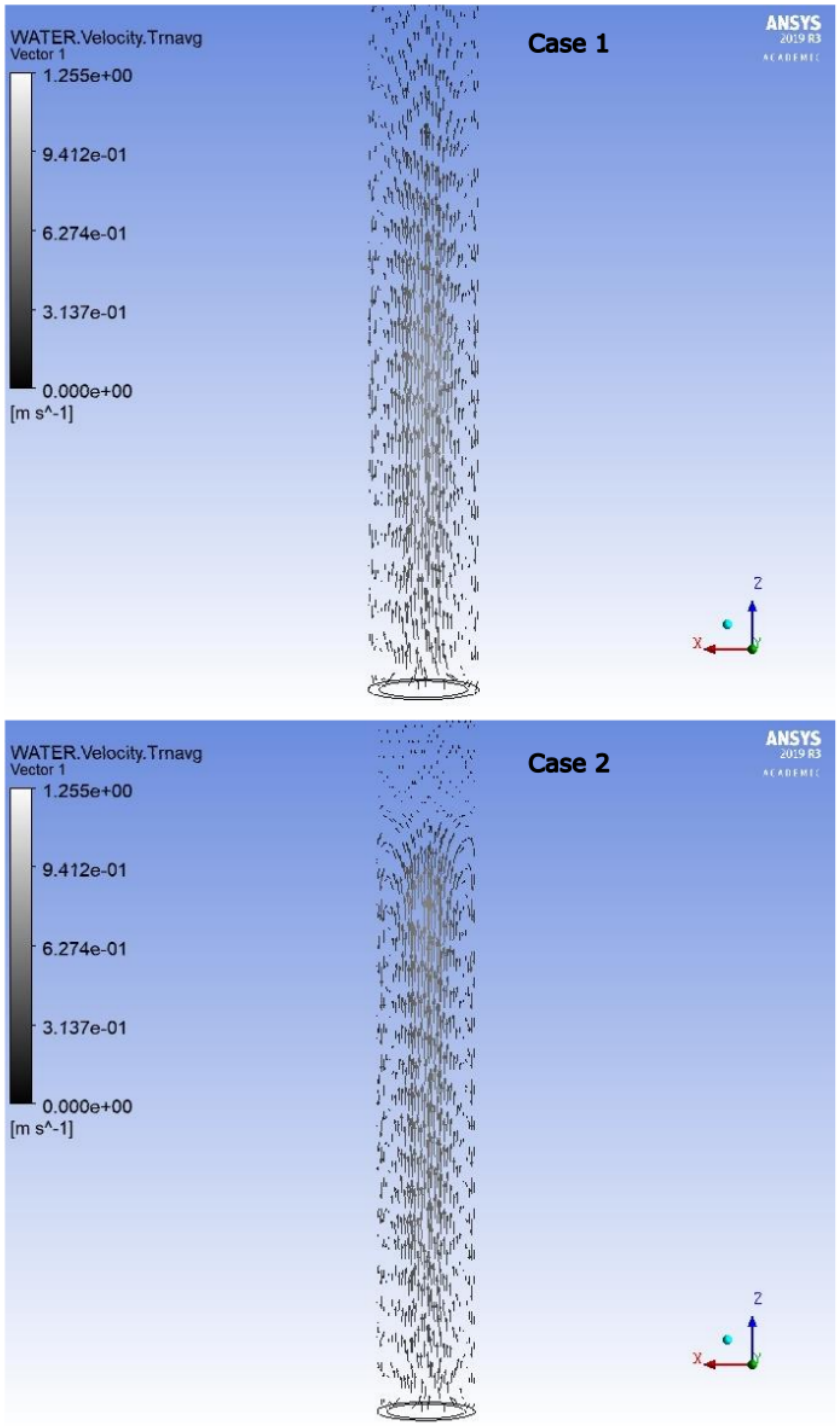


Figure 5: Vector plot of time-averaged water velocity for case 1 and case 2

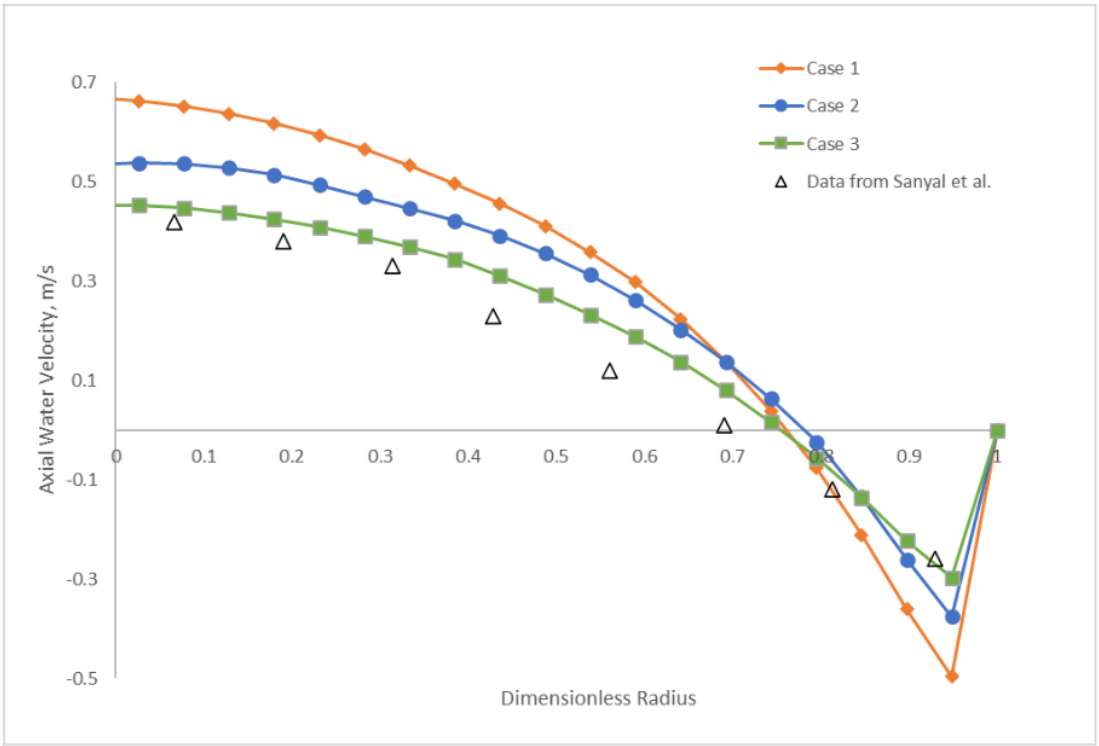


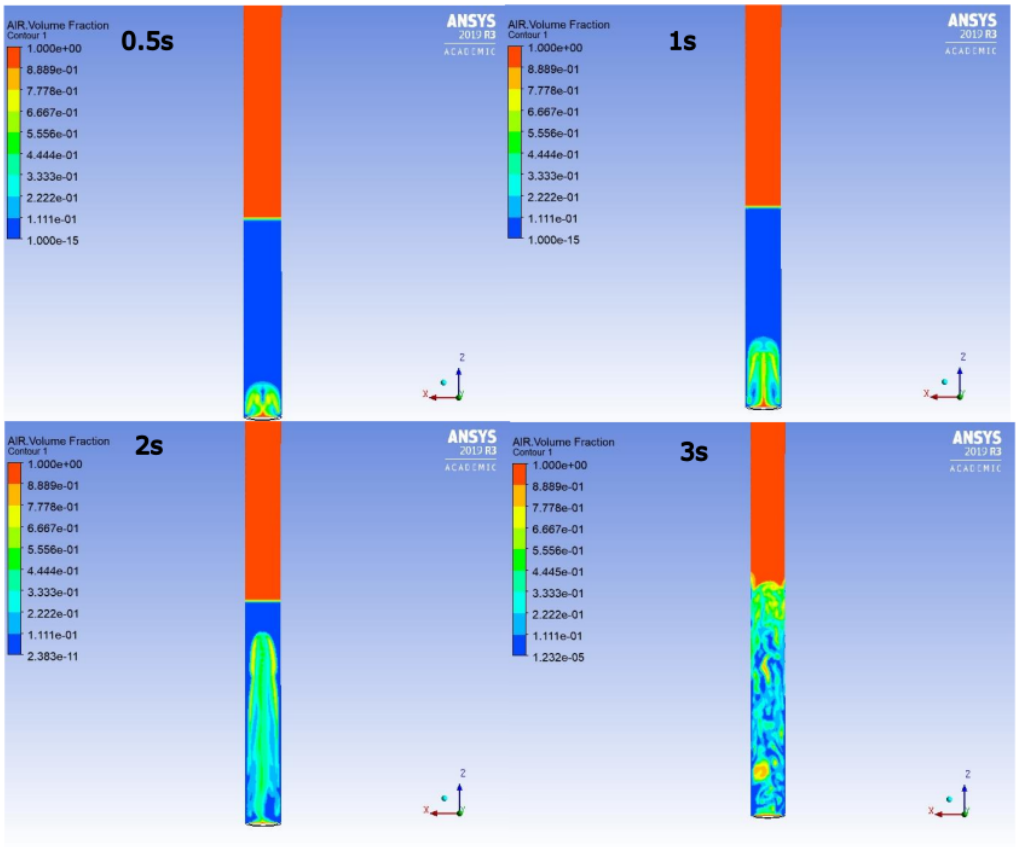
Figure 6: Comparison of axial water velocity profiles

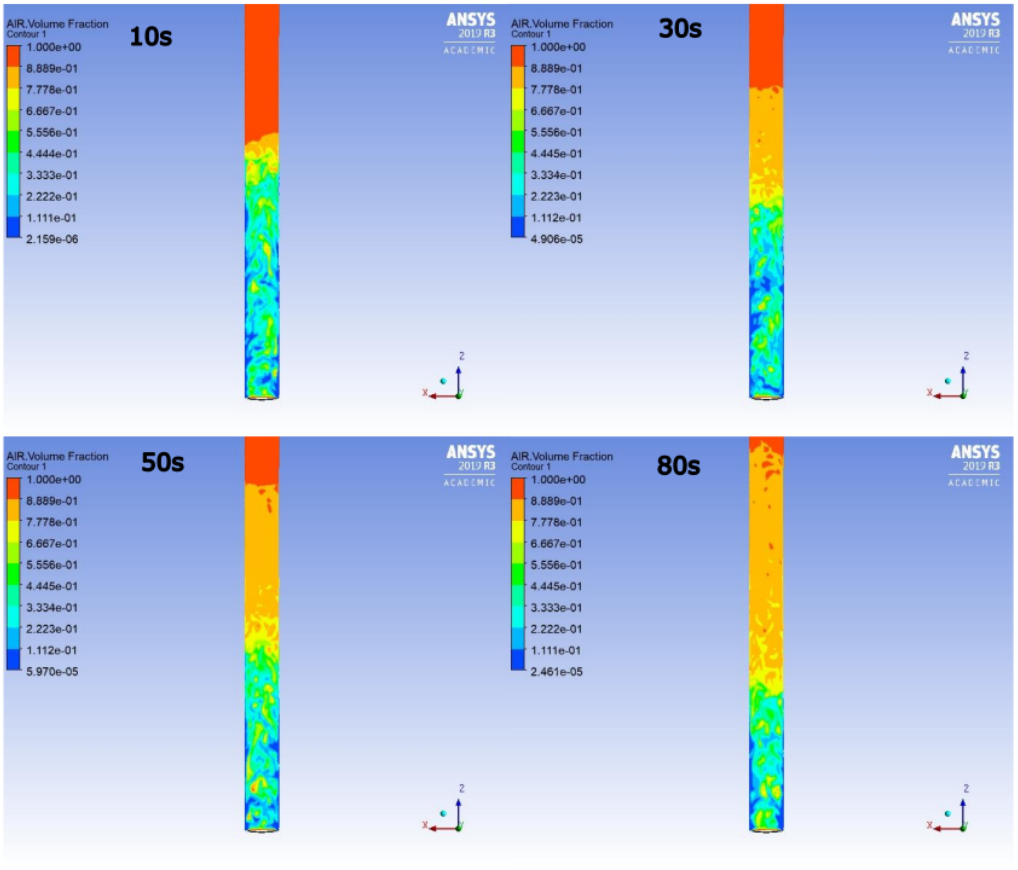
In *figure 6*, the time averaged axial water velocity distribution of three cases along the radial direction compared with experimental data from Sanyal et al. *[12]* is shown. As can be seen clearly from the figure, the axial water velocity from all three cases is overpredicted. However, the general shape of the profile is predicted well and the crossover point *(the radial location where the axial component of velocity is zero)* can be predicted quite well. Comparing *case 1 and case 2*, it can be seen that the case adopting Schiller Naumann drag force model is generally more consistent with the experimental results than the case adopting Ishii Zuber drag force model. The velocity profile of Ishii Zuber drag force model has the maximum variation. Comparing *case 2 and case 3*, an obvious optimization on the prediction of axial water velocity can be obtained when considering virtual mass force and lift force.

4.2 Radial Gas Holdup

Gas holdup is one of the basic parameters to characterize the hydrodynamic characteristics in the bubble column, and directly affects the mass transfer characteristics and reaction speed in the reactor. Therefore, it is of great significance to study and design the bubble column. *Figure series 7* below shows the transient gas holdup distribution of *case 1* in the central section of bubble column with time. The advantage of LES shown here is that LES is able to contain and show more transient details inside the flow field therefore the fully detailed condition in this figure can be obtained.

Figure series 7: Gas hold up of case 1 with time





After the initial intake *(0.5s-2s)*, the bubble is subject to a large resistance from the liquid, so a wide gas holdup distribution at the top of the bubble flow can be obviously observed. Since the bubble column is all liquid phase at the initial time, when the bubble flow moves to the liquid level, the bubbles will break up and enter the atmosphere above the liquid level, and only a small part will be dispersed in the liquid phase through reflux. In the bubble tower, the gas phase exists in the continuous liquid phase in the form of dispersed bubbles. With the development of time, the gas holdup distribution widens, which is mainly due to the increase of liquid turbulence caused by bubble flow movement, intensifying the fluid backflow at the liquid level and promotes the distribution of gas phase in the liquid phase. On

the other hand, the bubbles coalesce in the rising movement, which makes the main body of the bubble flow wider.

The connection between gas hold up and axial water velocity is that the distribution of gas holdup results in a lower static pressure distribution in the central region than the pressure near the wall, and a stronger circulating flow developed in the flow area flows upward at the centre and downward near the tower wall. However, it should be clear that the flow pattern described here is the flow pattern after a long period of average. Instantaneous flow forms consist of a series of flow structures of different sizes and shapes that do not usually remain static in time and space, which has been illustrated in the previous part *4.1*.

Figure 8 shows the time averaged radial gas holdup distribution of three cases along the radial direction compared with experimental data from Sanyal et al. *[12]*.

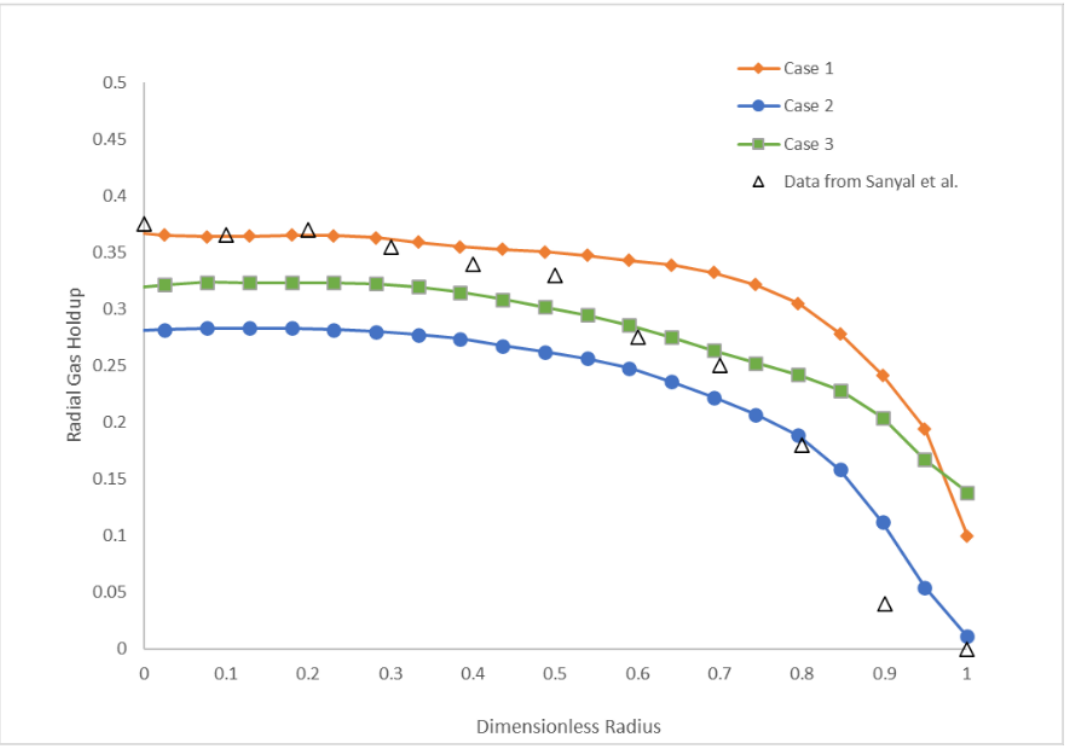


Figure 8: Time averaged gas hold up

From *figure 8,* it can be seen that in a turbulent state, despite success in capturing the general shape of the gas hold up distribution profile, there are still some differences between the two models, and the data seem to be included in the prediction range. The approximate parabola shape observed in the experimental data can also be observed through the simulation results. The increasing gas volume fraction in the centre of the column causes the liquid to move upward at high speed due to the buoyancy of the gas, while the liquid in the batch state moves downward around the column. Comparing *Case 1 and Case 2*, Ishii Zuber drag force model predicts more accurately when it is near the centre and Schiller Naumann predicts the distribution well when it is near the wall. *Case 3* predicts well along the middle of them.

5. Conclusion

Large eddy simulation has been carried out for the cylindrical bubble column and three cases are separately set up considering different interfacial forces to be compared with the experimental data from Sanyal et al. *[12]*. *Case 1* adopts Ishii Zuber drag force model and chooses to neglect lift force and virtual mass force. *Case 2* adopts Schiller Naumann drag force model and chooses to neglect lift force and virtual mass force. *Case 3* adopts Schiller Naumann drag force model, considering the effects of lift force and virtual mass force. Tomiyama model is adopted to describe the lift force. The following conclusions can be drawn from the research results:

(1) LES model can capture the details of fluid transient flow, which provides a more comprehensive understanding of bubble column.

(2) All three cases can capture the general shape of the both water velocity and gas holdup distribution profile.

(3) An obvious optimization on the prediction of axial water velocity can be obtained when considering virtual mass force and lift force.

(4) Proper consideration of various interfacial forces is the key to the success of the simulation.

Statement:

Dear Sir,

Sorry for late submission of this dissertation. I was found to get a fever and acute gastritis on 25th May and sent to hospital for Covid-19 examination. I was under insulated for one week and because of this, I was not able to go back to my dormitory to get my laptop. I also could not go to the PC room in SEB to have access to the computer cluster where my simulations were run. That makes my dissertation cannot be finished on time. The EC application has been approved and the new deadline is 24th June. Thanks all the teachers that support me during the application!

Best regards,

Ziyan WU

References:

1. Shu, S. L., Vidal, D., Xiong, Q. G., Bertrand, F., Chaouki, J. *Multiscale Multiphase Phenomena in Bubble Column Reactor: A Comprehensive Review*. Particuology PARTIC-D-18-00106.

2. Zhang D., Deen N. G., Kuipers J. A. M. *Numerical simulation of dynamic flow behavior in a bubble column: a study of closures for turbulence and interface forces*. Chemical Engineering Science, 2006, 61: 7593-7608.
3. Krishna R., Sie S. T. *Design and Scale-up of the Fischer−Tropsch Bubble Column Slurry Reactor[J]*. Fuel Process. Technol., 2000, 64(1): 73−105.
4. Shah Y. T. *Reaction engineering in direct coal liquefaction*. USA: Addison-Wesley., 1981.
5. Kuipers J. A. M., van Swaaij W. P. M., *Application of computational fluid dynamics to chemical reaction engineering*. Review in Chemical Engineering, 1997, 13: 1-118.
6. Krishna R., van Baten J. M., Ureanu M. I. *Three-phase Eulerian simulations of bubble column reactors operating in the churn-turbulent regime: a scale up strategy*. Chemical Engineering Science, 2000, 55:3275-3286.
7. Mudde R. F., Simonin O. *Two and three dimensional simulation of a bubble plume using a two fluid model*. Chemical Engineering Science, 1999, 54:5061-5071.
8. Li G., Yang X. G., Dai G. C. *CFD Simulation of Effects of the Configuration of Gas Distributors on Gas−Liquid Flow and Mixing in a Bubble Column [J]*. Chem. Eng. Sci., 2009, 64(24): 5104−5116.
9. Pfleger D., Becker S. *Modelling and Simulation of the Dynamic Flow Behaviour in a Bubble Column [J]*. Chem. Eng. Sci., 2001, 56(4): 1737−1747.
10. Muhammad A. A., Moses O. T., Vishnu K. P. *Two-fluid Eulerian Simulation of Bubble Column Reactors with Distributors [J]*. J. Chem. Eng. Jap., 2006, 39(8): 831−841.

11. Zhang D., Deen N. G., Kuipers J. A. M. *Numerical Simulation of the Dynamic Flow Behavior in a Bubble Column: A Study of Closures for Turbulence and Interface Forces [J]*. Chem. Eng. Sci., 2006, 61(23): 7593−7608.
12. Sanyal J., Vasquez S., Roy S., Dudukovic M. P. *Numerical simulation of gas-liquid dynamics in cylindrical bubble column reactors*. Chemical Engineering Science, 1999,54: 5071-5083.
13. Bao J. K. *Numerical Simulation of Transient Characteristics in Bubble Column Reactors*. Tianjin University, 2004, TQ05.
14. Deen N. G., *Large eddy simulation of the Gas-Liquid flow in a square cross-sectioned bubble column*. Chemical Engineering Science, 2001, 56: 6341~6349.
15. Smagorinsky J., *General circulation experiments with the primitive equations*. The basic experiment, Month. Wen. Rev., 1963, 91: 99~164.
16. Lilly D. K., *On the application of the eddy viscosity concept in the inertial subrange of turbulence*. NCAR Manuscript, 1966, 123.
17. Shur M.L., Spalart P.R., Strelets M.K., Travin A.K., *A hybrid RANS-LES approach with delayed-DES and wall-modeled LES capabilities*. Int. J. Heat Fluid Flow, 2008, 29: 1638–1649.
18. Sato Y., Sadatomi M., Sekoguchi K., *Momentum and heat transfer in twophase bubble flow—I. Theory*. Int. J. Multiph. Flow, 1981, 7 (2): 167–177.
19. Ma T., Ziegenhein T., Lucas D., Krepper, E., Frohlich J., *Euler-Euler large eddy simulations for dispersed turbulent bubbly flows*. International Journal of Heat and Fluid Flow, 2015, 56:51-59.
20. Ishii, M., Zuber N. *Drag coefficient and relative velocity in bubbly, droplet or particulate flows*. AIChE Journal, 1979, 25:843-855.

21. Schiller L, Naumann A. *A Drag Coefficient Correlation [J]*. Vdi Zeitung, 1935, 77: 318−320.

22. Tomiyama, A. *Transverse migration of single bubbles in simple shear flows[J]*. Chemical Engineering Science, 2002, 57:1849-1858.

23. Buwa V., Ranade V. *Dynamics of gas-liquid flow in a rectangular bubble column: experiments and single/multi-group CFD simulations[J]*. Chem. Eng. Sci., 2002, 57:4751-4736.

24. Cook T. L., Harlow F. H. *Vortices in bubbly two-phase flow[J]*. Int. J. Multiphase Flow, 1986, 12(1) :35-61.

25. Stewart H. B., Wendroff B., *Two-phase flow: Models and methods,* Journal of Computational Physics, 1984, 56: 363-409.

26. Jakobsen H. A., Sannaes B. H., *Modelling of vertical bubble-driven flows,* Industrial and Engineering Chemistry Research, 1997, 36: 4052-4074.

Ziyan_WU 6521805

GRADEMARK REPORT

FINAL GRADE

/100

GENERAL COMMENTS

Instructor

PAGE 1

PAGE 2

PAGE 3

PAGE 4

PAGE 5

PAGE 6

PAGE 7

PAGE 8

PAGE 9

PAGE 10

PAGE 11

PAGE 12

PAGE 13

PAGE 14

PAGE 15

PAGE 16

PAGE 17

PAGE 18

PAGE 19

PAGE 20

PAGE 21

PAGE 22

PAGE 23

PAGE 24

PAGE 25

PAGE 26

PAGE 27

PAGE 28

PAGE 29

PAGE 30

PAGE 31

PAGE 32